



Analysing certain protein kinase inhibitors used in cancer research comparative using QSAR analysis

Garima

Assistant Professor, Department of Chemistry, Om Sterling Global University, Hisar, Haryana, India

Abstract

Protein kinase inhibitors play a crucial role in cancer research and treatment. Protein kinases are enzymes that regulate various cellular processes by catalyzing the transfer of phosphate groups from ATP to specific target proteins, thereby modulating their activity. Dysregulation of protein kinases is a common feature in many types of cancer, making them attractive targets for therapeutic intervention. The inhibitors employed in this work for the comparative analysis include PLK1, CK1 delta, ATM, LRRK2, and LRRK2. These inhibitors are all very useful in the treatment of cancer.

Keywords: Kinetochore, alzheimer's, circadian, hypertension

Introduction

Polo Like Kinase 1 (PLK1)

Protein kinase has emerged as a key target for cancer-related therapy discovery in the twenty-first century. PLKs are a family of five members that go by the names PLK1–5. The primary modulator of mitotic progression is a member of the ser/thr protein kinase family called PLKs (Polo Like Kinases). Their structure is made up of single or double polo boxes in the conserved catalytic domains at the C and N terminals. Of these, PLK1 is the most dominant member of the family in proliferating cells because it is overexpressed in numerous tumours, including endometrial, gastric, prostatic, breast, ovarian, head, neck, and pancreatic cancers. PLK1 is involved in the maturation of centrosomes, spindle formation, cytokinesis, and kinetochore.

While PLK2 and PLK3 are not highly expressed in proliferating cells, PLK1 is highly elevated during mitosis. PLK5 might not be involved in the advancement of the cell cycle since it lacks a kinase domain. Therefore, it is crucial to create PLK1 inhibitors with homologous specificity. The reduction of PLK1 enzymatic activity by small drugs has made PLK1 an important aspect in cancer therapy. This can be achieved by obstructing the catalytic domain and by considering the possibility for neoplastic alteration of the enzyme [1-5].

Receptor Interacting Protein Kinase 2 (RIPK2)

NOD (nucleotide binding and oligomerization domain) signalling is mediated by RIPK2. The binding process leads to the activation of the MAP (mitogen-activated protein kinase) and nuclear factor kB (NF-kB) pathways, which in turn promotes the transcription of proinflammatory cytokines. Both of these routes are essential in the case of pathological disorders such as multiple sclerosis, Crohn's disease, and inflammatory bowel disease. NODs (NOD1, NOD2) are helpful in determining diseases that are resistant to antibiotics. Furthermore, RIPK2 is strongly involved in breast cancer and oral squamous cell tumours. In stomach cancer nerves, the third most common major cause of cancer-related mortality worldwide, RIPK2 is overexpressed in messenger RNA and protein levels.

RIPK2 can be extremely important in GC therapy by controlling the proliferation of GC cells through NF-kB

signalling regulation. The third line of treatment for chronic myeloid leukaemia is ponatinib. The FDA (Food and Drug Administration) has approved the cancer medication ponatinib, which is a recognised RIPK2 inhibitor. This multi-kinase inhibitor mainly targets BCR-ABL, a fusion protein made up of the sequences of the ABL protein and the BCR gene. Owing to its multitargeted uses, this medication is used to treat a variety of cancers, including gastrointestinal stromal tumours, thyroid, breast, and lung cancers. It's an inhibitor of several kinases. There exists a correlation between RIPK2 activities and advanced tumour, metastasis, body mass index (BMI), and group stages.

A ser/thr protein kinase, RIPK2 is involved in the activation of NF-kB and caspase-mediated cell death, a type of programmed cell death. It has a CARD (C-terminal caspase and recruitment domain) and an N-terminal kinase along with a transitional segment. The seven protein kinases that make up the RIPK family are homologous to the serine-threonine/tyrosine kinase domain. Because it contains a protein that interacts with DD of TNF (tumour necrosis factor) receptor superfamily member six, RIPK2 is referred to as the death domain. The most thoughtful family members are RIPK1-3. RIPK4-RIPK6 are involved in immunity and inflammation. RIPK7 is a mucosal defence protein. Receptor interacting protein-2, or RIPK2, is the primary term for RIPK2. In 1998, equivalency studies against the kinase domain of RIPK1 led to the simulation of CARD domains, which are now known as RIPK2 [6-10].

Casein kinase 1(CK1) delta

The two families of casein kinases (CK), CK1 and CK2, are a group of ser/thr kinases that are expressed in eukaryotes. CK1 is widely expressed as the ser/thr protein kinase family in organisms that have been shown to phosphorylate a broad range of proteins. In various biological processes, such as DNA repair, cell division, apoptosis, Alzheimer's disease, and circadian rhythm, CK1 homologues are essential. The CK1 family has seven isotypes in humans and many other species: ϵ , δ , η_3 , η_2 , η_1 , β , and α . Neurodegenerative illnesses and cancer are treated with CK1 inhibitors.

In many cellular functions, trafficking, cytoskeleton maintenance, Wnt signalling, cancer, and circadian rhythm, serine/threonine kinase CK1 delta is essential. Different

types of cancer are promoted by CK1 delta. Numerous illnesses, including ovarian, glioblastoma, colorectal, chronic lymphocytic leukaemia, breast malignancies, and pancreatic adenocarcinomas, can be treated by targeting CK1 delta. Although they exhibit changes in the size and primary structure of the N and C terminal domains, all of these distinct isoforms exhibit remarkable preservation in their catalytic domains.

Several members of the CK1 family implicated in various illnesses. CK1 delta is implicated in Parkinson's and Alzheimer's disease. The alpha isoform of CK1 is implicated in hepatitis C. Both the delta and the epsilon isotypes are implicated in family advanced sleep phase problems. Alpha, delta, and epsilon are the three isoforms that are implicated in leishmaniasis and tumours. Wnt signalling, a complex network of signal transduction pathways controlling various developmental processes in addition to tissue homeostasis and primary development, is a well-known cellular mechanism that is regulated by CK1 delta [11-15].

Ataxia Telangiectasia Mutated (ATM)

In 1995, Ataxia Telangiectasia Mutated gene was identified with the development of ataxia telangiectasia mutated syndrome disease. This gene is found in the chromosomes and contains about 66 neurites that encode a PI3K-related ser/thr protein kinase. In the DNA repair and response system, Ataxia Telangiectasia Mutated kinase plays a very important role. ATM kinase, which is the primary and initial transducer involved in double-strand breaks (DSBs). Ataxia-telangiectasia(A-T) is a genetic disorder altered by the ATM protein that is a product of the gene. The human diseases group from which A-T belongs are jointly known as 'genetic instability syndromes'. A-T also known as Louis - Bar syndrome is a rare autosomal receding syndrome, the patient suffering from this exhibit a wide range of irregularities like premature aging, insulin resistance, ataxia, neurodegeneration, increase sensitivity towards ionizing radiation, telangiectasia, variable immunodeficiencies and predisposition to cancer. ATM kinase contributes to maintaining genome integrity in DNA double-strand breaks. After activation, ATM kinase is used to phosphorylate many substrates like KAP1, Akt Cck2 and p53 used in many cellular control processes like DNA repair, cell-cycle control, survival and cell-apoptosis. Ataxia Telangiectasia mutated patients lacking ATM gene mutation are categorized by thymic degeneration, genome instability, predisposition to cancer and immunodeficiency. Reliably, the deficiency of ATM kinase connects with sensitivity to ionizing chemical-induced or radiation-induced DNA damage, especially I and II inhibitors of DNA topoisomerase.

The ATM (Ataxia Telangiectasia Mutated) kinase belongs to the phosphatidylinositol 3-kinases (PI3K-like kinases) family. It controls and regulates various processes, including gene expression, cell metabolism, stress response and intracellular group. ATM kinase belongs to the preserved family of proteins. ATM is a ser/thr protein kinase [16-20].

Leucine-rich repeat kinase 2(LRRK2)

In the year 1817, a scientist named James Parkinson described a disease known as Parkinson's disease (PD). It is the most common neurodegenerative disorder. It is a neurodegenerative brain disorder characterized by four

fundamental motor indications: postural instability, bradykinesia, rigidity and resting tremor. A number of nonmotor indications are, however, progressively recognized as being portion of the illness manifestation. These include constipation, hyposmia, problems with speech, mood disorders and swallowing, cognitive impairment, orthostatic hypertension, and sleep disorders.

In the year 2004, it is found that alterations in LRRK2 can be the key cause of Parkinson's disease. Even not a single alteration of LRRK2, in fact diversity of inherent ties to this illness. The popular mutation of LRRK2 is Gly2019Ser or G2019S, are noticed in patients with autosomal leading PD and in those with outward irregular PD, who are clinically indistinguishable from those with idiopathic PD. Typical of multifactorial illnesses, the existence of PD rises with age, with a predictable 0.3% distressed at age 50 increasing to 4.3% by age of 85. This mutation lies in a preserved part of the protein kinase domain that starts the activation loop, which, as the name suggests, normalizes catalytic enzyme activity. PD results in neuronal disfunction and advanced loss of dopamine-producing neurons situated in the substantia nigra pars compacta area of the midbrain. Foremost among these are mitochondrial dysfunction, autophagy/lysosomal dysfunction, and inflammation, all of which are highly combined and complexly controlled. The detection of pathogenic LRRK2 alterations in 2004 opened a new opening for PD therapy, with a focus on emerging LRRK2 inhibitors. However, drug expansion has established to be highly challenging with absence of knowledge concerning LRRK2 biology, blood-brain barrier (BBB) permeability restriction, and a lack of preclinical models that authentically summarize PD phenotypes, among many stimulating factors that need to be overcome to advance drugs for potential first-in-human hearings. Numerous LRRK2 inhibitors have been described, but many of the them deficiency of selectivity or the capability to pass the blood-brain barrier. One of the most promising and actively pursued targets for the forthcoming pharmaceutical action of PD is LRRK2. Huge efforts are being made in this area from the academic community and the pharmaceutical sector with the goal of developing selective and brain-permeable LRRK2 inhibitors as a treatment for Parkinson's disease. Furthermore, multiple investigations revealed that LRRK2 the amount of -synuclein that aggregates in dopaminergic neurons exposed to -synuclein fibrils have been found increased by mutations. Drug virtual screening or optimisation heavily rely on QSAR/QSPR modelling, which has emerged as one of the core computational molecular modelling technique. QSAR models make it possible to pinpoint connections between a physicochemical or biological feature under investigation and the structural details of chemical substances (molecular descriptors). These techniques are frequently employed in place of experimental research nowadays to envisage the activity of molecules grounded on their structure. Particularly, over the past few decades, machine learning techniques have seen widespread use in this discipline. A minimal amount of QSAR investigations in LRRK2 have been available in the scholarly literature. In addition to this, the majority of research papers revealed a little predictive activity for the datasets used for external validation. The information and findings reported in a conference article presented at the 12th International Conference on Practical Applications of Computational Biology & Bioinformatics are extended in

that paper with new QSAR models for envisaging potential inhibitors of the LRRK2 protein. Specifically, a number of regression and classification QSAR models are compared for accuracy and model complexity, along with their accuracy performances [6]. LRRK2 also exhibits GTPase activities, playing a crucial role in the regulation of intracellular processes. Leucine-rich repeat kinase 2 (LRRK2) is located on human chromosome 12 with 51 exons and encodes a protein of 286 kDa. Over-expression of mutant LRRK2 has been found to be toxic in neurons. Many studies have been undertaken to screen the mutation of this gene in several specific regions, in order to design inhibitors for suppressing PD and LRRK2 toxicity in neurons. One of the most repetitive mutations in LRRK2 occurs in the G2019S substitution, and is attracting growing attention to target LRRK2 toxicity by creating specific inhibitors targeting this site. Several approaches have been developed to design various LRRK2 inhibitors to treat PD [21-25].

Dataset I

The present work has developed a reliable QSAR model from a dataset of 68 tetrahydropteridin derivatives. The

developed QSAR model is robust statistically and has good predictive quality.

Model: (Divided dataset)

$$pIC_{50} = 6.5142(\pm 2.9651) + 11.4495(\pm 6.1553) \times \max HaaCH - 0.0307(\pm 0.0112) \times ATSC7i - 0.1573(\pm 0.0369) \times AATS7m$$

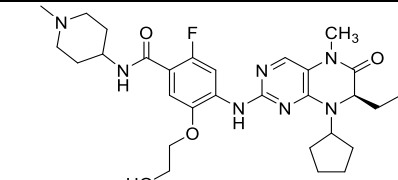
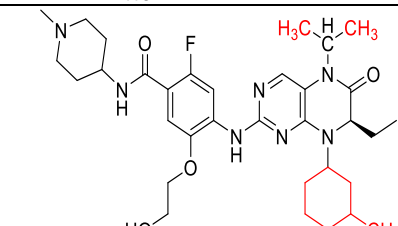
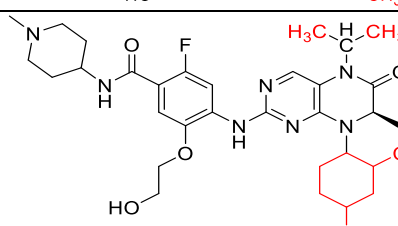
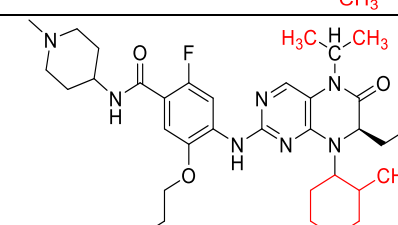
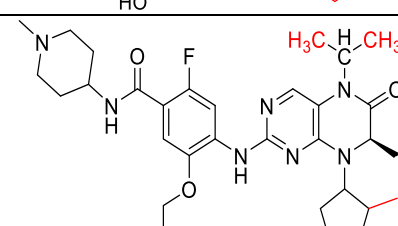
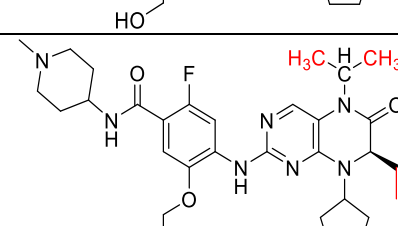
The numerical values of different statistical parameters are 0.8213, 0.8091, 0.7841, 0.8771, and 0.9364 for R^2 , R^2_{adj} , Q^2_{loo} , R^2_{ext} , and CCC_{ext} , respectively. (Table 6.1) Using the result of the QSAR model, five compounds (D1-D5) were also designed. A molecular docking study of the most active compound (L28) and designed compounds (D1-D5) was done to find the best interaction between protein and ligand. The docking results found that the designed compounds showed similar pattern of interaction as that of the most active compound (L28). Hence, the results of the present investigation may be employed to identify and develop effective inhibitors for the treatment of PLK1-related pathophysiological disorders.

Table 1: Values of Statistical parameters as obtained from QSAR model

Statistical parameters	Result	Statistical parameters	Result
N_{tr}	48	No. of descriptors	3
N_{ex}	20	θ^*	-2.2602°
Fitting Criteria			
R^2_{tr}	0.8213	RMSE _{tr}	0.3656
R^2_{adj}	0.8091	MAE _{tr}	0.3054
$R^2_{tr} - R^2_{adj}$	0.0122	RSS _{tr}	6.4144
LOF	0.1745	CCC _{tr}	0.9019
Kxx	0.413	s	0.3818
ΔK	0.1507	F	67.3877
Internal Validation Criteria		External Validation Criteria	
$R^2_{cv}(Q^2_{loo})$	0.7841	RMSE _{ext}	0.3091
$R^2 - Q^2_{loo}$	0.0371	MAE _{ext}	0.2249
RMSE _{cv}	0.4017	PRESS _{ext}	1.9114
MAE _{cv}	0.3354	R^2_{ext}	0.8771
PRESS _{cv}	7.7464	$Q^2 - F^1$	0.8771
CCC _{cv}	0.8821	$Q^2 - F^2$	0.8744
Q^2_{LMO}	0.7731	$Q^2 - F^3$	0.8722
R^2_{Yscr}	0.0644	CCC _{ext}	0.9364
Q^2_{Yscr}	-0.1165	R^2_m aver.	0.8218
RMSE ^{AV} _{Yscr}	0.836	R^2_m delta	0.0261
Predictions by LOO			
Exp(x) vs. Pred(y)		Pred(x) vs. Exp(y)	
R^2	0.7848	R^2	0.7848
R^2_o	0.7404	R^2_o	0.7842
k'	0.9976	k	0.9993
Clos'	0.0565	Clos	0.0008
R^2_m	0.6195	R^2_m	0.7654
External predictions by model equation			
Exp(x) vs. Pred(y)		Pred(x) vs. Exp(y)	
R^2	0.8771	R^2	0.8771
R^2_o	0.871	R^2_o	0.8748
k'	1.0004	k	0.9977
Clos'	0.0069	Clos	0.0026
R^2_m	0.8087	R^2_m	0.8349

Table 2: Predicted pIC_{50} of the designed compounds with their structure and binding affinity

S. No.	Structure	Predicted pIC_{50}	Binding affinity (kcal/mol)
--------	-----------	----------------------	-----------------------------

L28		8.22	-7.92
I.D1		8.91	-8.23
I.D2		9.31	-8.27
I.D3		9.47	-8.28
I.D4		9.50	-8.92
I.D5		10.62	-9.00

Dataset II

In this study, the QSAR model was developed by taking a dataset of 50 pyrimidine and pyridine derivatives. QSAR model was reliable and robust.

Model: (Divided dataset)

$$\begin{aligned}
 pIC_{50} = & -11.2408(\pm 0.0022) + \\
 & 0.5838(\pm 0.1507) \times C1SP2 + \\
 & 7.3064(\pm 3.7111) \times (Spmin3_Bhp) + \\
 & 1.5709(\pm 0.8691) \times AATS4p - \\
 & 0.2851(\pm 0.1953) \times C3SP2 + \\
 & 6.7788(\pm 1.4509) \times (VE1_Dt) + \\
 & 1.4513(\pm 0.6517) \times GATS8c
 \end{aligned}$$

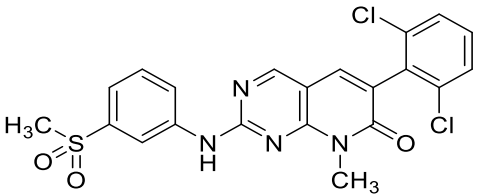
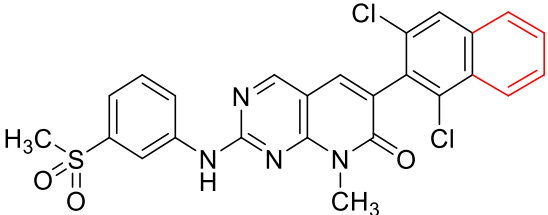
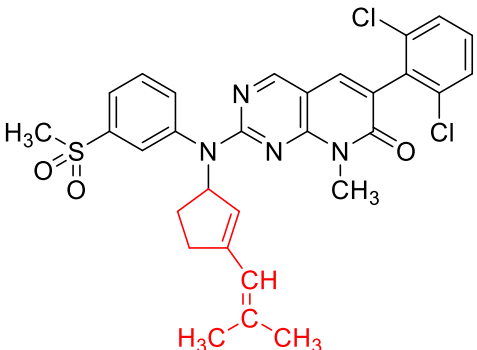
The values obtained from model with six descriptors had good predictive potential. This model's statistical parameters

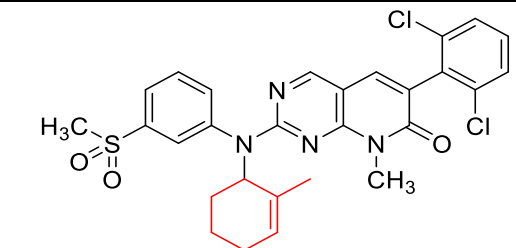
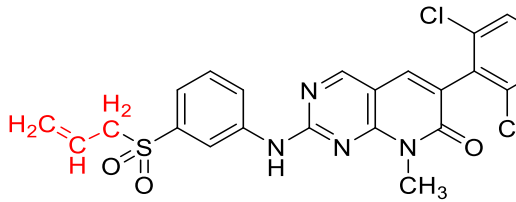
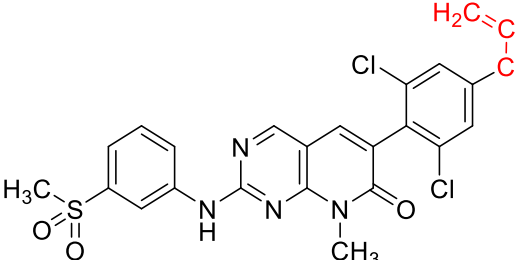
values were 0.8550, 0.8269, 0.7993, 0.8532, 0.903 for R^2 , R^2_{adj} , Q^2_{loo} , R^2_{ext} , and CCC_{ext} respectively. (Table 6.3) To find the best protein-ligand interaction, a molecular docking study was done. A molecular docking study of the most active compound (SN30) and designed compounds (E1-E5) was done to find the best interaction between protein and ligand. The docking results found that the designed compounds showed similar pattern of interaction as that of the most active compound (SN30). The docking results found that the most potent compound forms H-bonding with GLN150 and SER102. The hydrophobic interactions were shown by MET98, ALA45, LEU79, LYS47, ALA163, LEU153 and LEU24 all these residues. With the help of results obtained from QSAR model five compounds named as E1-E5 were designed.

Table 3: Statistical parameters for the developed model of RIPK2 inhibitors

Statistical parameters	Result	Statistical parameters	Result
N_{tr}	38	No. of descriptors	6
N_{ex}	12	θ^*	1.0032°
Fitting Criteria		External Validation Criteria	
R^2_{tr}	0.855	$RMSE_{tr}$	0.1762
R^2_{adj}	0.8269	MAE_{tr}	0.1398
$R^2_{tr} - R^2_{adj}$	0.0281	RSS_{tr}	1.1803
LOF	0.0663	CCC_{tr}	0.9218
Kxx	0.386	s	0.1951
ΔK	0.0041	F	30.4612
Internal Validation Criteria		External Validation Criteria	
$R^2_{cv}(Q^2_{loo})$	0.7993	$RMSE_{ext}$	0.1228
$R^2 - Q^2_{loo}$	0.0557	MAE_{ext}	0.1064
$RMSE_{cv}$	0.2073	$PRESS_{ext}$	0.1808
MAE_{cv}	0.1671	R^2_{ext}	0.8532
$PRESS_{cv}$	1.6337	$Q^2 - F^1$	0.8458
CCC_{cv}	0.8923	$Q^2 - F^2$	0.7776
Q^2_{LMO}	0.781	$Q^2 - F^3$	0.9296
R^2_{Yscr}	0.1649	CCC_{ext}	0.903
Q^2_{Yscr}	-0.2663	R^2_m aver.	0.761
$RMSE^{AV}_{Yscr}$	0.4223	R^2_m delta	0.1401
Predictions by LOO		Pred(x) vs. Exp(y)	
Exp(x) vs. Pred(y)		Pred(x) vs. Exp(y)	
R^2	0.8005	R^2	0.8005
R'^2_o	0.7678	R'^2_o	0.7993
k'	0.9993	k	1
Clos'	0.0408	Clos	0.0015
R'^2_m	0.6558	R'^2_m	0.7727
External predictions by model equation			
Exp(x) vs. Pred(y)		Pred(x) vs. Exp(y)	
R^2	0.8532	R^2	0.8532
R'^2_o	0.8525	R'^2_o	0.8171
k'	1.0066	k	0.9933
Clos'	0.0008	Clos	0.0424
R'^2_m	0.8311	R'^2_m	0.691

Table 4: Predicted pIC_{50} of the designed compounds with their structure and binding affinity

S.No.	Structure	Predicted pIC_{50}	Binding affinity(kcal/mol)
SN30		8.221849	-9.36
II.E1		9.252623	-10.46
II.E2		9.169523	-10.42

II.E3		9.095514	-10.38
II.E4		8.965639	-9.66
II.E5		8.255452	-9.62

Dataset III

In this study QSAR model for 51 compounds of *N*-(benzothiazolyl)-2-phenyl-acetamides derivatives and benzothiazoles derivatives were developed. The model obtained with three descriptors was statistically robust and reliable.

Model: (Divided dataset)

$$pIC_{50} = 8.7296(\pm 0.6355) + 0.179(\pm 0.07) \times RDF95v - 2.7183(0.5553) \times GATS7i - 4.9056(\pm 2.6917) \times RotBFrac$$

The values of statistical parameter for this model were 0.8217, 0.8060, 0.7843, 0.8265 and 0.8916 for R^2 , R^2_{adj} , Q^2_{loo} , R^2_{ext} , and CCC_{ext} respectively. (Table 6.5) To find the

best protein-ligand interaction, a molecular docking study was done. A molecular docking study of the most active compound (34S) and designed compounds (F1-F4) was done to find the best interaction between protein and ligand. The docking results found that the designed compounds showed similar pattern of interaction as that of the most active compound (34S). Some compounds (F1-F4) were created based on the molecular modelling methods used in this investigation (Table 6.6). The machine learning techniques employed in this work subsequently predicted the inhibitory potential (pIC_{50}) of these compounds (Table 6.6).

Table 5: Statistical parameters of the QSAR model obtained for CK1 delta inhibitor

Statistical parameters	Result	Statistical parameters	Result
N_{tr}	38	No. of descriptors	3
N_{ex}	13	θ^*	2.6903°
Fitting Criteria			
R^2_{tr}	0.8217	$RMSE_{tr}$	0.3283
R^2_{adj}	0.806	MAE_{tr}	0.2656
$R^2_{tr} - R^2_{adj}$	0.0157	RSS_{tr}	4.0967
LOF	0.152	CCC_{tr}	0.9021
Kxx	0.3364	s	0.3471
ΔK	0.1018	F	52.2381
Internal Validation Criteria		External Validation Criteria	
$R^2_{cv}(Q^2_{loo})$	0.7843	$RMSE_{ext}$	0.3803
$R^2 - Q^2_{loo}$	0.0374	MAE_{ext}	0.3148
$RMSE_{cv}$	0.3612	$PRESS_{ext}$	1.8804
MAE_{cv}	0.2947	R^2_{ext}	0.8265
$PRESS_{cv}$	4.9565	$Q^2 - F^1$	0.744
CCC_{cv}	0.8814	$Q^2 - F^2$	0.7327
Q^2_{LMO}	0.7727	$Q^2 - F^3$	0.7608
R^2_{Yscr}	0.0829	CCC_{ext}	0.8916
Q^2_{Yscr}	-0.151	$R^2_{m\ aver.}$	0.664
$RMSE^{AV}_{Yscr}$	0.7442	$R^2_{m\ delta}$	0.1802
Predictions by LOO			
Exp(x) vs. Pred(y)		Pred(x) vs. Exp(y)	
R^2	0.7847	R^2	0.7847

R^2_o	0.7379	R^2_o	0.7843
k'	0.9961	k	1.0004
$Clos'$	0.0596	$Clos$	0.0005
R^2_m	0.615	R^2_m	0.7691
External predictions by model equation			
Exp(x) vs. Pred(y)		Pred(x) vs. Exp(y)	
R^2	0.8265	R^2	0.8265
R^2_o	0.8188	R^2_o	0.7331
k'	0.9936	k	1.0024
$Clos'$	0.0093	$Clos$	0.113
R^2_m	0.7541	R^2_m	0.5739

Table 6: Predicted pIC₅₀ of the designed compounds with their structure and binding affinity

S.No.	Structure	Predicted pIC ₅₀	Binding energy(kcal/mol)
34S		8.0	-6.97
III.F1		8.8643	-8.15
III.F2		8.7100	-8.12
III.F3		8.5936	-7.94
III.F4		8.0635	-7.14

Dataset IV

In this study QSAR model for 68 compounds which are derivatives of quinolines carboxamides derivatives and imidazo[5,4-c] quinolin-2-one scaffold is selected for the QSAR model development. The model obtained with three descriptors was statistically robust and reliable.

Model: (Divided dataset)

$$pIC_{50} = 3.2365 - 1.8997(\pm 0.8396) \times \text{minHdsCH} + 0.0005(\pm 0.0003) \times \text{ATSC6v} + 0.3956(\pm 0.0805) \times \text{SpMAD_Dzp}$$

The values of statistical parameter for this model were 0.8727, 0.8642, 0.8501, 0.9251 and 0.9452 for R^2 , R^2_{adj} , Q^2_{loo} , R^2_{ext} , and CCC_{ext} respectively. (Table 6.7) A molecular docking study of the most active compound

(K47) and designed compounds (G1-G5) was done to find the best interaction between protein and ligand. The docking results found that the designed compounds showed similar pattern of interaction as that of the most active compound (K47). It was inferred from the observation that the hydrogen bonding takes place between amino acid residue THR1043 and most active ligand. HIS708 and ARG

707 forms hydrophobic interactions with the most potent compound. Some compounds (G1-G5) were created based on the molecular modelling methods used in this investigation (Table 6.8). The machine learning techniques employed in this work subsequently predicted the inhibitory potential (pIC_{50}) of these compounds (Table 6.8).

Table 7: Results of statistical parameters for ATM inhibitors

Statistical parameters	Result	Statistical parameters	Result
N_{tr}	49	No. of descriptors	3
N_{ex}	19	θ^*	2.3188°
Fitting Criteria			
R^2_{tr}	0.8727	$RMSE_{tr}$	0.4895
R^2_{adj}	0.8642	MAE_{tr}	0.4066
$R^2_{tr} - R^2_{adj}$	0.0085	RSS_{tr}	11.7411
LOF	0.3111	CCC_{tr}	0.932
Kxx	0.3302	s	0.5108
ΔK	0.1884	F	102.8224
Internal Validation Criteria		External Validation Criteria	
$R^2_{cv}(Q^2_{loo})$	0.8501	$RMSE_{ext}$	0.34
$R^2 - Q^2_{loo}$	0.0226	MAE_{ext}	0.2323
$RMSE_{cv}$	0.5312	$PRESS_{ext}$	2.1966
MAE_{cv}	0.4421	R^2_{ext}	0.9251
$PRESS_{cv}$	13.8244	$Q^2 - F^1$	0.875
CCC_{cv}	0.9202	$Q^2 - F^2$	0.8743
Q^2_{LMO}	0.8452	$Q^2 - F^3$	0.9386
R^2_{Yscr}	0.0598	CCC_{ext}	0.9452
Q^2_{Yscr}	-0.1175	R^2_m aver.	0.7958
$RMSE^{AV}_{Yscr}$	1.3299	R^2_m delta	0.0877
Predictions by LOO			
Exp(x) vs. Pred(y)		Pred(x) vs. Exp(y)	
R^2	0.8503	R^2	0.8503
R^2_o	0.8301	R^2_o	0.8501
k'	0.9955	k	0.9992
Clos'	0.0238	Clos	0.0003
R^2_m	0.7295	R^2_m	0.8376
External predictions by model equation			
Exp(x) vs. Pred(y)		Pred(x) vs. Exp(y)	
R^2	0.9251	R^2	0.9251
R^2_o	0.9166	R^2_o	0.8901
k'	0.9813	k	1.0171
Clos'	0.0092	Clos	0.0379
r^2_m	0.8397	r^2_m	0.752

Table 8: Predicted pIC_{50} of the designed compounds with their structure and binding affinity

S.No.	Structure	Predicted pIC_{50}	Binding energy(kcal/mol)
K47		9.769551	-8.13
IV.G1		10.23327	-11.00

IV.G2		10.12959	-9.33
IV.G3		9.926531	-9.31
IV.G4		9.89689	-9.28
IV.G5		9.833472	-8.66

Dataset V

In this study QSAR model for 58 compounds of pyrrolo[2,3-b] pyridines, Pyrrolo[2,3-d] pyrimidines, and Pyrrolo[3,2-c] pyridine were taken into consideration for developing QSAR model. The model obtained with three descriptors was statistically robust and reliable.

Model: (Divided dataset)

$$pIC_{50} = -4.0857(\pm 2.4307) + 0.0145(\pm 0.0092) \times ATSC7i - 0.0007(\pm 0.0003) \times ATSC8v + 1.4898(\pm 0.357) \times piPC7$$

The values of statistical parameter for this model were 0.8261, 0.8120, 0.7769, 0.7998 and 0.8941 for R^2 , R^2_{adj} , Q^2_{loo} , R^2_{ext} , and CCC_{ext} respectively. (Table 6.9) A molecular docking study of the most active compound (D21026) and designed compounds (H1-H5) was done to find the best interaction between protein and ligand. The docking results found that the designed compounds showed

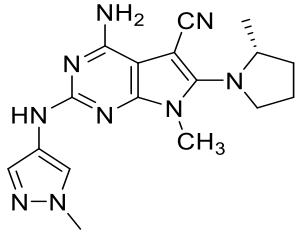
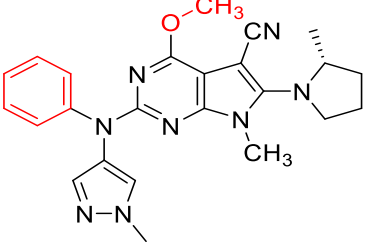
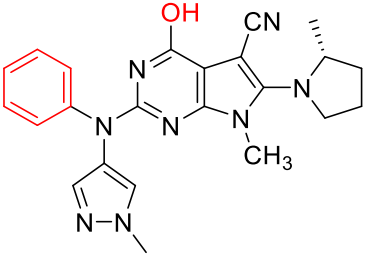
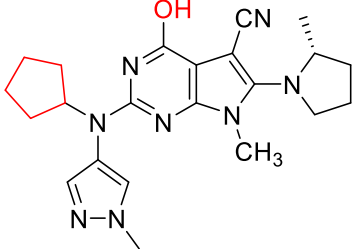
similar pattern of interaction as that of the most active compound (D21026). The hydrophobic contact between different amino acid residues, including LYS 38, MET 84, ALA 147, LEU 59, and the most effective molecule D21026, was deduced from the fact that this interaction occurs. Molecular docking was used to clarify the binding mechanism of the most effective drug, D21026, within the active site of 7BK2 following the successful validation of the docking procedure. Through the hydrogen of the OH group, the most powerful molecule, D21026, forms a hydrogen bond with the important residue GLU 17. Some compounds (H1-H5) were created based on the molecular modelling methods used in this investigation (Table 6.10). The machine learning techniques employed in this work subsequently predicted the inhibitory potential (pIC_{50}) of these compounds (Table 6.10).

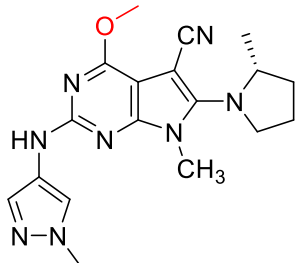
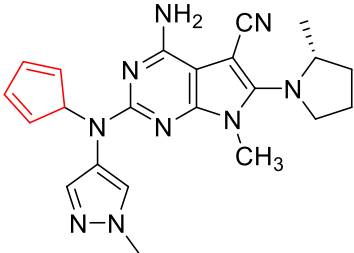
Table 9: Values of statistical parameters obtained from QSAR model

Statistical parameters	Result	Statistical parameters	Result
N_{tr}	41	No. of descriptors	3
N_{ex}	17	θ^*	-2.6018°
Fitting Criteria			
R^2_{tr}	0.8261	RMSE _{tr}	0.4249
R^2_{adj}	0.812	MAE _{tr}	0.3603
$R^2_{tr} - R^2_{adj}$	0.0141	RSS _{tr}	7.4023
LOF	0.2478	CCC _{tr}	0.9048
Kxx	0.2472	s	0.4473
ΔK	0.2102	F	58.5977

Internal Validation Criteria		External Validation Criteria	
$R^2_{cv}(Q^2_{loo})$	0.7769	RMSE _{ext}	0.4674
$R^2 - Q^2_{loo}$	0.0492	MAE _{ext}	0.3711
RMSE _{cv}	0.4813	PRESS _{ext}	3.7139
MAE _{cv}	0.4052	R^2_{ext}	0.7998
PRESS _{cv}	9.4984	$Q^2 - F^1$	0.784
CCC _{cv}	0.88	$Q^2 - F^2$	0.7837
Q^2_{LMO}	0.7701	$Q^2 - F^3$	0.7896
R^2_{Yscr}	0.0776	CCC _{ext}	0.8941
Q^2_{Yscr}	-0.1368	R^2_m aver.	0.7161
RMSE ^{AV} _{Yscr}	0.9782	R^2_m delta	0.0321
Predictions by LOO			
Exp(x) vs. Pred(y)		Pred(x) vs. Exp(y)	
R^2	0.7789	R^2	0.7789
R'^2_o	0.7414	R'^2_o	0.7769
k'	0.9952	k	0.9996
Clos'	0.0481	Clos	0.0025
R'^2_m	0.6281	R'^2_m	0.7443
External predictions by model equation			
Exp(x) vs. Pred(y)		Pred(x) vs. Exp(y)	
R^2	0.7998	R^2	0.7998
R'^2_o	0.7926	R'^2_o	0.7842
k'	0.9985	k	0.9967
Clos'	0.009	Clos	0.0195
R'^2_m	0.7321	R'^2_m	0.7

Table 10: Predicted pIC_{50} of the designed compounds with their structure and binding affinity

S.No.	Structure	Predicted pIC_{50}	Binding energy(kcal/mol)
D21026		8.301	-6.97
V.H1		9.424953	-8.91
V.H2		8.531437	-8.77
V.H3		8.439507	-8.40

V.H4		8.332397	-7.83
V.H5		8.322227	-7.52

Conclusion

It is clear from all the datasets that protein kinase inhibitors are highly helpful in the research of cancer. The reduction of PLK1 enzymatic activity by small drugs has made PLK1 an important aspect in cancer therapy. There exists a correlation between RIPK2 activities and advanced tumour, metastasis, body mass index (BMI), and group stages. According to all of them, RIPK2 is an analytical marker for both progressive phase breast cancer and inflammatory breast cancer (IBC). Numerous illnesses, including ovarian, glioblastoma, colorectal, chronic lymphocytic leukaemia, breast malignancies, and pancreatic adenocarcinomas, can be treated by targeting CK1 delta.

The family of phosphatidylinositol 3-kinases, or PI3K-like kinases, includes the ATM (Ataxia Telangiectasia Mutated) kinase protein. Numerous functions, such as gene expression, cell metabolism, stress response, and intracellular group, are regulated and controlled by it. The physiological role of LRRK2 and some of its substrates are unknown. Nevertheless, a number of LRRK2 inhibitors are used to treat Parkinson's disease (PD) in a neuroprotective manner, and it has been suggested that they could help prevent neurodegeneration. It can be inferred that all of these inhibitors can be employed in the creation of different cancer medications.

References

- Li Z, Xu L, Zhu L, Zhao Y, Hu T, Yin B, *et al.* Design, synthesis and biological evaluation of novel pteridinone derivatives possessing a hydrazone moiety as potent PLK1 inhibitors. *Bioorg. Med. Chem. Lett*,2020;30(16):127329.
- Duchowicz PR. Linear Regression QSAR Models for Polo-Like Kinase-1 Inhibitors. *Cells*,2018;7(2):13.
- Bhujbal S, Keretsu S, Cho S. A Combined Molecular Docking and 3D-QSAR Studies on Tetrahydropteridin Derivatives as PLK2 Antagonists. *Bull. Korean Chem. Soc*, 2019, 40.
- Shahin R, Al Hashimi NN, Daoud NeH, Aljamal S, Shaheen O. QSAR-guided pharmacophoric modeling reveals important structural requirements for Polo kinase 1 (Plk1) inhibitors. *J. Mol. Graph. Model*,2021;109:108022.
- Chekkara R, Kandakatla N, Gorla VR, Tenkayala SR, Susithra E. Theoretical studies on benzimidazole and imidazo[1,2-a]pyridine derivatives as Polo-like kinase 1 (Plk1) inhibitors: Pharmacophore modeling, atom-based 3D-QSAR and molecular docking approach. *J. Saudi Chem. Soc*,2017;21:S311-S321.
- SJ Humphrey, DE James, M Mann. Protein Phosphorylation: A Major Switch Mechanism for Metabolic Regulation, *Trends in Endocrinol. Metab*,2015;26:676-687. doi: <https://doi.org/10.1016/j.tem.2015.09.013>
- JA Ubersax, JE Ferrell Jr. Mechanisms of specificity in protein phosphorylation, *Nat. Rev. Mol. Cell Biol*,2007;8:530-541. doi: 10.1038/nrm2203
- C Suebsuwong, D Pinkas, S Ray, J Bufton, B Dai, A Bullock, *et al.* Activation loop targeting strategy for design of receptor-interacting protein kinase 2 (RIPK2) inhibitors, *Bioorganic Med. Chem. Lett*, 2018, 28. doi: 10.1016/j.bmcl.2018.01.044
- SR Hofmann, L Girschick, R Stein, F Schulze. Immune modulating effects of receptor interacting protein 2 (RIP2) in autoinflammation and immunity, *Clin. Immunol*,2021;223:108648. doi: <https://doi.org/10.1016/j.clim.2020.108648>
- Q Yang, S Tian, Z Liu, W Dong. Knockdown of RIPK2 Inhibits Proliferation and Migration, and Induces Apoptosis via the NF- κ B Signaling Pathway in Gastric Cancer, *Front. Genet*, 2021, 12. doi: 10.3389/fgene.2021.627464
- EL Mazzoldi, A Pastò, E Ceppelli, G Pilotto, V Barbieri, A Amadori, *et al.* Casein Kinase 1 Delta Regulates Cell Proliferation, Response to Chemotherapy and Migration in Human Ovarian Cancer Cells, *Frontiers in Oncology*, 2019, 9. doi: 10.3389/fonc.2019.01211
- IG Salado, M Redondo, ML Bello, C Perez, NF Liachko, BC Kraemer, *et al.* Protein Kinase CK-1 Inhibitors as New Potential Drugs for Amyotrophic Lateral Sclerosis, *Journal of Medicinal Chemistry*,2014;57:2755-2772. doi: 10.1021/jm500065f
- A Spinaci, M Buccioni, D Catarzi, C Cui, V Colotta, D Dal Ben, *et al.* "Dual Anta-Inhibitors" of the A2A Adenosine Receptor and Casein Kinase CK1delta: Synthesis, Biological Evaluation, and Molecular Modeling Studies, *Pharmaceuticals*,2023;16:167. doi:

14. K Joshi, S Goyal, S Grover, S Jamal, A Singh, P Dhar, *et al.* Novel group-based QSAR and combinatorial design of CK-1 δ inhibitors as neuroprotective agents, *BMC Bioinformatics*,2016;17:515. doi: 10.1186/s12859-016-1379-9
15. FR Makhuri, JB Ghasemi. Computer-aided scaffold hopping to identify a novel series of casein kinase 1 delta (CK1d) inhibitors for amyotrophic lateral sclerosis, *European Journal of Pharmaceutical Sciences*,2015;78:151-162. doi: <https://doi.org/10.1016/j.ejps.2015.07.011>
16. SA Armstrong, CW Schultz, A Azimi Sadjadi, JR Brody, MJ Pishvaian. ATM Dysfunction in Pancreatic Adenocarcinoma and Associated Therapeutic Implications, *Mol Cancer Ther*,2019;18:1899-1908. doi: 10.1158/1535-7163.MCT-19-0208
17. Y Shiloh. ATM and related protein kinases: safeguarding genome integrity, *Nat Rev Cancer*,2003;3:155-68. doi: 10.1038/nrc1011
18. A Guleria, S Chandna. ATM kinase: Much more than a DNA damage responsive protein, *DNA Repair (Amst)*,2016;39:1-20. doi: 10.1016/j.dnarep.2015.12.009
19. X Dou, X Sun, H Huang, L Jiang, Z Jin, Y Liu, *et al.* Discovery of novel ataxia telangiectasia mutated (ATM) kinase modulators: Computational simulation, biological evaluation and cancer combinational chemotherapy study, *Eur J Med Chem*,2022;233:114196. doi: 10.1016/j.ejmech.2022.114196
20. J Chwastek, D Jantas, W Lason. The ATM kinase inhibitor KU-55933 provides neuroprotection against hydrogen peroxide-induced cell damage via a gammaH2AX/p-p53/caspase-3-independent mechanism: Inhibition of calpain and cathepsin D, *Int J Biochem Cell Biol*,2017;87:38-53. doi: 10.1016/j.biocel.2017.03.015
21. Paisan Ruiz C, Lewis PA, Singleton AB. LRRK2: cause, risk, and mechanism. *J Parkinsons Dis*,2013;3(2):85-103.
22. Tolosa E, Vila M, Klein C, Rascol O. LRRK2 in Parkinson disease: challenges of clinical trials. *Nat Rev Neurol*,2020;16(2):97-107.
23. Mata IF, Wedemeyer WJ, Farrer MJ, Taylor JP, Gallo KA. LRRK2 in Parkinson's disease: protein domains and functional insights. *Trends Neurosci*,2006;29(5):286-93.
24. Atashrazm F, Dzamko N. LRRK2 inhibitors and their potential in the treatment of Parkinson's disease: current perspectives. *Clin Pharmacol*,2016;8:177-189.
25. Gilsbach BK, Messias AC, Ito G, Sattler M, Alessi DR, Wittinghofer A, *et al.* Structural Characterization of LRRK2 Inhibitors. *J Med Chem*,2015;58(9):3751-6.